

AD 655211

SIMPLE CLASSICAL MODEL FOR THE SCATTERING OF
GAS ATOMS FROM A SOLID SURFACE: *
ADDITIONAL ANALYSES AND COMPARISONS

R. M. Logan, J. C. Keck, and R. E. Stickney
Department of Mechanical Engineering and
Research Laboratory of Electronics
Massachusetts Institute of Technology
Cambridge, Massachusetts

Abstract

The simple classical model for the scattering of gas atoms from a solid surface as described recently by Logan and Stickney [J. Chem. Phys. 44, 195 (1966)] is further developed and the basic assumptions are examined in detail. The analysis is modified so that a closed-form expression is obtained for the angular distribution of the scattered atoms. With this expression it is possible to identify the principal parameters of the model. The theoretical results are in qualitative agreement with recent experimental data for the scattering of a molecular beam from a solid surface. A closed-form expression is also obtained for the dependence of the velocity distribution of the scattered atoms on the angle of scattering. The analysis is extended to include, in an approximate manner, the effects of surface roughness and a square-well gas-surface potential.

Nomenclature

- M = Mass of gas atom
- m = Mass of surface atom
- μ = Mass ratio M/m
- T_g = Temperature of gas beam

* This work was supported by the Joint Services Electronics Program under Contract DA36-039-AMC-03200(E). Computations were made at the M.I.T. Computation Center.

T	= Temperature of surface
θ_o^s	= Incident angle, measured from surface normal
θ_1	= Outgoing angle, measured from surface normal in plane of incident beam and normal
u_o	= Incident gas velocity (normal component u_{no})
u_1	= Outgoing gas velocity (normal component u_{n1})
\bar{u}	= Mean incident normal gas velocity
v_o^{no}	= Relative velocity of gas and surface atoms
v_o^R	= Velocity (normal to surface) of surface atom before collision
$F_o(u_o)$	= Normalized velocity distribution in incident beam
$G_o(v_o)$	= Normalized velocity distribution of surface atoms
B_1	= $\frac{1+\mu}{2} \sin \theta_o \cot \theta_1 - \frac{1-\mu}{2} \cos \theta_o$
B_2	= $\frac{1+\mu}{2} \sin \theta_o \operatorname{cosec}^2 \theta_1$
B_3	= $\sin \theta_1 / \sin \theta_o$

I. Introduction

Recently we proposed and analyzed a simple classical model for the scattering of gas atoms from a solid surface.¹ Since the theoretical results were shown to agree surprisingly well with the general, qualitative features of existing experimental data, we suggest that this elementary model may provide a valid base for the development of a more exact scattering theory. The purpose of the present paper is to investigate and improve the original model by identifying the principal parameters, examining the underlying assumptions, computing additional properties, and making further comparisons of theory with experiment.

The basic assumptions of the model are summarized as follows:

(1) Both the gas atoms and surface atoms are represented by rigid elastic particles (i.e., the intermolecular potential is impulsive).

(2) Collisions with the surface do not change the tangential component of the gas atom (i.e., the surface is perfectly smooth).

(3) The surface atoms are represented by independent particles confined by a square-well potential.

(4) The velocity distribution of the surface atoms is assumed to be Maxwellian.

Figure 1 aids in the description of the model and the analysis. A gas atom of mass M , velocity u_o , and angle of incidence θ_o collides with a surface atom of mass m and velocity v_o , and it is scattered with velocity u_1 at angle θ_1 . Since the tangential component u_{to} is unchanged according to assumption (2), only the change u_{no} in the normal component need be considered. It follows from assumption (1) that an expression for u_{n1} , the normal velocity component of the scattered gas atom, may be derived simply from the classical mechanics of rigid, elastic bodies,

$$u_{n1} = \frac{1 - \mu}{1 + \mu} u_{no} + \frac{2}{1 + \mu} v_o \quad (1)$$

where μ is the mass ratio, M/m . With this knowledge of u_{n1} we may now determine θ_1 by using an expression derived from the geometry shown in Fig. 1:

$$\cot \theta_1 = (u_{n1}/u_{no}) \cot \theta_o \quad (2)$$

Since Eqs. (1) and (2) enable one to determine θ_1 for any combination of u_{no} and v_o , an expression for the scattering pattern (i.e., the angular distribution) may be derived for any choice of distribution functions for u_{no} and v_o .

II. Closed-Form Expression for Scattering Pattern

In reference 1 two methods of analysis of the model were described. The first was an approximate method based on mean speeds; this gave a closed-form result, but only for the position of the maximum of the scattering pattern. The second method yielded the full scattering pattern, but numerical integration was necessary. A third method is now presented in which a closed-form expression for the complete scattering pattern is obtained.

We assume that the fraction of gas atoms having double (or multiple) collisions with the surface is negligible. This is a good assumption over a wide range of practical conditions, as is seen from Fig. 4 of reference 2. Furthermore, it is unlikely that the simple model considered here can correctly deal with double collisions. Under these conditions the differential rate at which collisions occur between incident gas atoms and surface atoms is given by

$$d^2R = V_{R_o} F_o(u_o) G_o(v_o) du_o dv_o \quad (3)$$

The probability distribution for scattering is obtained by writing $v_o = v_o(u_o, \theta_1)$, integrating over u_o and dividing by the number of particles striking the surface per unit time \bar{u}_{no} :

$$\frac{1}{\bar{u}_{no}} \frac{dR}{d\theta_1} = \frac{1}{\bar{u}_{no}} \int_{u_o=0}^{\infty} v_o F_o(u_o) G_o(v_o) \left| \frac{\partial v_o}{\partial \theta_1} \right| du_o \quad (4)$$

By eliminating u_{n1} from Eqs. (1) and (2),

$$v_o = \left(\frac{1+\mu}{2} \sin \theta_o \cot \theta_1 - \frac{1-\mu}{2} \cos \theta_o \right) u_o \equiv B_1 u_o \quad (5)$$

Hence,

$$\left| \frac{\partial v_o}{\partial \theta_1} \right| = \left(\frac{1+\mu}{2} \sin \theta_o \csc^2 \theta_1 \right) u_o \equiv B_2 u_o \quad (6)$$

and

$$v_R = u_o \cos \theta_o + v_o = (\cos \theta_o + B_1) u_o \quad (7)$$

By using Eqs. (5), (6), and (7) in Eq. (4), we obtain

$$\frac{1}{\bar{u}_{no}} \frac{dR}{d\theta_1} = \frac{1}{\bar{u}_{no}} \int_{u_o=0}^{\infty} (\cos \theta_o + B_1) B_2 u_o^2 F_o(u_o) G_o(B_1 u_o) du_o \quad (8)$$

The Maxwellian velocity distribution for gas and surface atoms are

$$F_o(u_o) du_o = \frac{4}{\pi^{1/2}} u_o^2 \left(\frac{M}{2kT_g} \right)^{3/2} \exp\left(-\frac{Mu_o^2}{2kT_g} \right) du_o \quad (9)$$

$$G_o(v_o) dv_o = \left(\frac{m}{2\pi kT_s} \right)^{1/2} \exp\left(-\frac{mv_o^2}{2kT_s} \right) dv_o \quad (10)$$

By using Eqs. (9) and (10) in Eq. (8) and integrating, we obtain

$$\frac{1}{\bar{u}_{no}} \frac{dR}{d\theta_1} = \frac{3}{4} \left(\frac{mT_g}{MT_s} \right)^{1/2} B_2 (1+B_1 \sec \theta_o) \left(1 + \frac{mT_g}{MT_s} B_1^2 \right)^{-5/2} \quad (11)$$

This equation gives the probability for scattering into unit angular range at angle θ_1 . The scattering patterns given by this equation agree closely with those given by the full analysis in reference 1. It should be noted that Eq. (11) gives the angular distribution of the flux of gas atoms leaving the surface; in cases where the experimental detector measures the density of scattered atoms, an alternative expression should be used (i.e., Eq. (21) of Section III).

According to Eq. (11) the scattering behavior depends only on the parameters θ_0 , μ and MT_s/mT_g . In Fig. 2 we plot the position of the peak of the lobe against MT_s/mT_g for two values of θ_0 and $\mu = 0.37$ (corresponding to A on Ag). Some points from the corresponding experimental data of Saltsburg and Smith³ are shown on the same figure. While there seems to be significant qualitative agreement between theory and experiment, the actual agreement is not as good as in many of the cases considered in reference 1. This may be due to the fact that for μ as large as 0.37, a considerable fraction of the gas atoms have double collisions, and these have been neglected. Furthermore, the model does not take into account the possibility of more than one atom of the solid being involved in the collision. We note that the quantity $(MT_s/mT_g)^{1/2}$ corresponds to the ratio of the mean speed of the solid atom to that of the gas atom.

The fact that we have treated the surface atoms as confined to rigid boxes, rather than as particles with harmonic motion, could cause errors in the following two ways: (a) In the oscillator case the relevant velocity distribution to use in the analysis would be different from the simple one-dimensional Maxwellian $G(v_0)$; it would, however, be closely similar in form. (b) The probability of a double collision between the gas atom and a surface atom is different in the two cases because the motion of the surface atom after the first collision is different in the two cases. We consider, however, that the present model is inadequate to deal with double collisions, and thus there would be little advantage in this respect in introducing a harmonic oscillator.

III. Velocity Distribution of Scattered Atoms

At each value of the outgoing angle θ_1 , the scattered atoms will have some distribution of velocities. We now

calculate this velocity distribution using methods similar to those employed in Section II.

The probability for scattering into unit angular range at θ_1 and into unit velocity range at u_1 is obtained by differentiating Eq. (3) with respect to u_1 , giving

$$\frac{1}{\bar{u}_{no}} \frac{d^2 R}{d\theta_1 du_1} = \frac{1}{\bar{u}_{no}} v_{R F_o}(u_o) G_o(v_o) \left| \frac{\partial v_o}{\partial \theta_1} \right| \left| \frac{\partial u_o}{\partial u_1} \right| \quad (12)$$

where u_o and v_o must be written in terms of u_1 and θ_1 . Since the tangential velocity is unchanged, we have

$$u_o = (\sin \theta_1 / \sin \theta_o) u_1 \equiv B_3 u_1 \quad (13)$$

and

$$\left| \frac{\partial u_o}{\partial u_1} \right| = B_3 \quad (14)$$

By using Eqs. (13) and (14), together with Eqs. (5), (6), and (7), in Eq. (12), we obtain

$$\frac{1}{\bar{u}_{no}} \frac{d^2 R}{d\theta_1 du_1} = \frac{1}{\bar{u}_o \cos \theta_o} B_2 B_3^3 u_1^2 (\cos \theta_o + B_1) F_o(B_3 u_1) G_o(B_1 B_3 u_1) \quad (15)$$

By substituting from Eqs. (9) and (10), and introducing the dimensionless velocity

$$U = u_1 \left(\frac{M}{2kT_g} \right)^{1/2} ,$$

Equation (15) becomes

$$\frac{1}{\bar{u}_{no}} \frac{d^2 R}{d\theta_1 dU} = \frac{2}{\pi^{1/2}} \left(\frac{mT_g}{MT_s} \right)^{1/2} B_2 B_3^5 (1 + B_1 \sec \theta_o) U^4 \exp \left[-B_3^2 \left(1 + \frac{mT_g}{MT_s} B_1^2 \right) U^2 \right] \quad (16)$$

It can be shown that Eqs. (11) and (16) satisfy the condition

$$\frac{1}{\bar{u}_{no}} \int_0^\infty \frac{d^2 R}{d\theta_1 dU} dU = \frac{1}{\bar{u}_{no}} \frac{dR}{d\theta_1} .$$

The velocity distribution at any angle θ_1 , normalized with

respect to integration over velocity, is then given by

$$P_f(U) = \frac{d^2R/d\theta_1 dU}{dR/d\theta_1} = \frac{8}{3\pi^{1/2}} B_3^5 \left(1 + \frac{mT_g}{MT_s} B_1^2\right)^{5/2} U^4 \exp\left[-B_3^2 \left(1 + \frac{mT_g}{MT_s} B_1^2\right) U^2\right] \quad (17)$$

This last expression gives the velocity distribution of the flux of atoms leaving the surface at any angle θ_1 . The corresponding expression for the density of scattered atoms is obtained by dividing Eq. (17) by U and renormalizing with respect to velocity to give

$$P_d(U) = 2B_3^4 \left(1 + \frac{mT_g}{MT_s} B_1^2\right)^2 U^3 \exp\left[-B_3^2 \left(1 + \frac{mT_g}{MT_s} B_1^2\right) U^2\right] \quad (18)$$

The most probable velocity at any angle θ_1 , for either flux or density distribution, is obtained by setting the derivatives of Eqs. (17) or (18)

$$\text{(Flux)} \quad U_f^*(\theta_1) = 2^{1/2} \frac{1}{B_3} \left(1 + \frac{mT_g}{MT_s} B_1^2\right)^{-1/2} \quad (19)$$

$$\text{(Density)} \quad U_d^*(\theta_1) = \left(\frac{3}{2}\right)^{1/2} \frac{1}{B_3} \left(1 + \frac{mT_g}{MT_s} B_1^2\right)^{-1/2} \quad (20)$$

In Fig. 3 we show typical curves obtained from Eq. (17).

In experiments with modulated molecular beams it should be possible to measure, as a function of θ_1 , a velocity corresponding approximately to either U_f^* or U_d^* . No results would seem to have been published in this form, but in Fig. 4 we show typical curves of U_f^* versus θ_1 for various values of T_s/T_g . The existence of a maximum for each of these curves is explained by consideration of the following two opposing physical effects: (a) For a given incident velocity u_0 , those atoms which receive the greatest impulse from the surface, and hence have the greatest outgoing velocity, will lie closest to the normal. (b) For a given impulse from the surface, those atoms with the smallest incident velocity, and hence the smallest outgoing velocity, will lie closest to the normal.

It is also possible to define an energy accommodation coefficient as a function of θ_1 based on the velocity U_f^* . We do not consider this to be a useful parameter in this situation, however, particularly since it generally takes the values $\pm\infty$ when $T_s = T_g$.

For comparison with data from experiments using a density sensitive detector, an approximate expression for the scattering pattern is obtained by dividing Eq. (11) by U_f^* to give

$$\frac{1}{U_f^* \bar{u}_{no}} \frac{dR}{d\theta_1} = \left(\frac{mT_g}{MT_s} \right)^{1/2} B_2 B_3 (1 + B_1 \sec \theta_o) \left(1 + \frac{mT_g}{MT_s} B_1^2 \right)^{-2} \quad (21)$$

It is found that the qualitative behavior of the curves given by Eq. (21) is the same as that of the curves given by Eq. (11) under nearly all conditions. Equation (21) does not represent a normalized distribution.

IV. Gas-Surface Potential

The use of a "soft" repulsive potential, rather than an impulsive potential, between the gas atom and the surface atom would introduce many complications and uncertainties. It is relatively simple, however, to introduce a stationary potential well, which the gas atom falls into before collision and climbs out of after collision. Such a stationary potential well is fairly realistic, since the attractive potential is due mainly to long range forces averaged over many surface atoms.

Let the well depth be E , and let the subscript E denote quantities in the well. The scattering distribution is still given formally by Eq. (4). In this case Eq. (1) becomes

$$u_{nlE} = \frac{1-\mu}{1+\mu} u_{noE} + \frac{2}{1+\mu} v_o \quad (22)$$

where $u_{nlE} = \left(u_{nl}^2 + \frac{2E}{M} \right)^{1/2}$, etc. Eq. (2) still stands, and we obtain from Eqs. (2) and (22)

$$v_o = \frac{1+\mu}{2} \left(u_o^2 \sin^2 \theta_o \cot^2 \theta_1 + \frac{2E}{M} \right)^{1/2} - \frac{1-\mu}{2} \left(u_o^2 \cos^2 \theta_o + \frac{2E}{M} \right)^{1/2} \\ \equiv v_o(u_o). \quad (23)$$

In this case

$$V_R = u_{noE} + v_o \quad (24)$$

Proceeding as in Section II, and defining the dimensionless quantity $W = E/kTg$, we obtain

$$\frac{1}{u_{noE}} \frac{dR_E}{d\theta_1} = \frac{1}{u_{noE}} \left(\frac{1+\mu}{2} \right)^2 \frac{\csc^2 \theta_1 \cot \theta_1}{\cot^2 \theta_o \cos \theta_o} \int_{\left(W \frac{2kT_g}{M} \right)^{1/2}}^{\infty} u_{noE} \left(u_{noE}^2 - W \frac{2kT_g}{M} \right)^{1/2} \\ \times \left\{ 1 + \frac{u_{noE}}{\left[\left(u_{noE}^2 - W \frac{2kT_g}{M} \right) \frac{\cot^2 \theta_1}{\cot^2 \theta_o} + W \frac{2kT_g}{M} \right]^{1/2}} \right\} F_o \left[u_o(u_{noE}) \right] G_o \left[v_o(u_{noE}) \right] du_{noE} \quad (25)$$

Scattering patterns are shown in Fig. 5 for the conditions $\theta_o = 45^\circ$, $T_s/T_g = 2.0$, $\mu = 0.02$, and $W = 0.0, 1.0$ and 10.0 . It is seen that the effect of increasing W is to shift the peak of the lobe towards the normal and to broaden the pattern.

V. Surface Roughness

We now eliminate assumption 2 (Section I) by introducing a surface roughness into the model. It immediately becomes necessary to consider a full three-dimensional scattering pattern rather than the somewhat artificial two-dimensional patterns. We use the coordinate system shown in Fig. 6, referring to θ as the in-plane angle and to ϕ as the out-of-plane angle. The xy -plane represents the ideal flat surface, and the angles α_x and α_y measure the deviation from a flat surface at any x point. y We characterize the over-all surface roughness by the normalized distribution functions $\rho_1(\alpha_x)$ and $\rho_2(\alpha_y)$.

In comparing the theory with experimental data in this case it is important to consider certain aspects of the detection system. For example, if the detector, which presumably subtends a small in-plane angle, subtends a large ($\sim 25^\circ$) out-of-plane angle, then it effectively integrates over the out-of-plane scattering. The extent of this effect will clearly depend on the relative widths of the detector and the out-of-plane scattering. Since the

theoretical expression is different for the cases with and without integration, it is important to know the details of the detector geometry. It is important to observe that the analysis in the previous sections assumes integration over the out-of-plane angle.

Proceeding as in Section II, the probability of scattering into unit solid angle at position (θ, ϕ) is given by

$$\frac{1}{\bar{u}_{no}} \frac{d^2R}{d\theta d\sin\phi} = \frac{1}{\bar{u}_o \cos\theta_o \cos\phi} \int \int_0^{\infty} V_R F_o(u_o) G_o(v_o) \rho_1(\alpha_x) \rho_2(\alpha_y) \left| \frac{\partial v_o}{\partial \theta} \frac{\partial \alpha_y}{\partial \phi} \right| du_o d\alpha_x \quad (26)$$

where v_o and α_y are written in terms of u_o and α_x . The extra $\cos\phi$ arises because the element of solid angle is $d\Omega = \cos\theta d\phi d\theta$. By assuming the coordinate rotations α_x and α_y are small, and keeping terms up to first order we obtain

$$\begin{aligned} v_o &= \left[\frac{1+\mu}{2} \sin\theta_o \cot\theta - \frac{1-\mu}{2} \cos\theta_o \right. \\ &\quad \left. + \alpha_x \left(\frac{1+\mu}{2} (\sin\theta_o \csc^2\theta + \cos\theta_o \cot\theta) + \frac{1-\mu}{2} \sin\theta_o \right) \right] u_o \\ &\equiv A_1(\alpha_x) u_o \end{aligned} \quad (27)$$

Similarly B_2 [Eq.(6)] becomes $A_2(\alpha_x)$ by differentiating Eq. (27). We also obtain

$$\alpha_y = \phi / (\cos\theta + \sin\theta \cot\theta_o) \equiv A_4 \phi \quad (28)$$

Hence Eq. (26) becomes

$$\frac{1}{\bar{u}_{no}} \frac{d^2R}{d\theta d\sin\phi} = \frac{1}{\bar{u}_o \cos\theta_o \cos\phi} \int \int [\cos\theta_o + A_1] A_2 u_o^2 F_o(u_o) G_o(A_1 u_o) \rho_1(\alpha_x) \rho_2(A_4 \phi) A_4 du_o d\alpha_x$$

The u_o integration may be carried out as in Eq.(11) to give

$$\frac{1}{\bar{u}_{no}} \frac{d^2 R}{d\theta dsin\phi} = \frac{1}{\cos\phi} \frac{3}{4} \left(\frac{mT_g}{MT_s} \right)^{1/2} \int_{\alpha_x} A_2 (1 + A_1 \sec\theta_o) \left(1 + \frac{mT_g}{MT_s} A_1^2 \right)^{-5/2} A_4 \rho_1(\alpha_x) \rho_2(A_4 \phi) d\alpha_x \quad (29)$$

We note that Eq. (29) contains an expression formally the same (with B's replaced by A's) as the flat surface distribution [Eq.(11)], multiplied by a term representing the roughness and integrated over α_x . To evaluate this integral, we take ρ_1 and ρ_2 as equal Gaussian distributions

$$\rho_1(\alpha) = \rho_2(\alpha) = \frac{1}{\sqrt{\pi} \langle \alpha \rangle} \exp \left(\frac{-\alpha^2}{\langle \alpha \rangle^2} \right)$$

and make the approximation

$$\left(1 + \frac{mT_g}{MT_s} A_1^2 \right)^{-5/2} \approx \exp \left(-\frac{5}{2} \frac{mT_g}{MT_s} A_1^2 \right) \quad (30)$$

Keeping terms to lowest order, we obtain

$$\frac{1}{\bar{u}_{no}} \frac{d^2 R}{d\theta dsin\phi} = -\frac{1}{\beta \sqrt{\pi}} e^{-\frac{\phi^2}{\beta^2}} \frac{3}{4} \sqrt{\frac{2}{5}} \left\{ e^{-\frac{B_1^2}{\gamma^2}} \frac{\partial}{\partial \theta} \left(\frac{B_1}{\gamma} \right) - \frac{1}{5} \frac{MT_s}{mT_g} \sec\theta_o \frac{\partial}{\partial \theta} \left(\gamma^{-1} e^{-\frac{B_1^2}{\gamma^2}} \right) \right\} \quad (31)$$

where

$$\beta^2 = \langle \alpha \rangle^2 (\cos\theta + \sin\theta \cot\theta_o)$$

$$\gamma^2 = \frac{2}{5} \frac{MT_s}{mT_g} + \langle \alpha \rangle^2 \sin^2\theta_o \left[1 + \frac{1+\mu}{2} \cot\theta (\cot\theta + \cot\theta_o) \right]^2$$

It may easily be verified that, for small values of β and γ , the integral of Eq. (31) over all angles is conserved and has the value of $3/4 \sqrt{2\pi/5} = 0.83$. The reason the value

is not unity, as it should be to conserve the total flux, is the result of the approximation Eq. (30) which falls off too rapidly for large B_1 .

For cases in which the detector is comparatively wide in the out-of-plane direction, we need to integrate Eq. (31) over the angle ϕ . The scattering distribution is then

$$\frac{1}{\bar{u}_{no}} \frac{dR}{d\theta} = -\frac{3}{4} \sqrt{\frac{2}{5}} \left[e^{-\frac{B_1^2}{\gamma^2}} \frac{\partial(B_1)}{\partial\theta} - \frac{1}{5} \left(\frac{MT_s}{mT_g} \right) \sec\theta_0 \frac{\partial}{\partial\theta} \left(\gamma^{-1} e^{-\frac{B_1^2}{\gamma^2}} \right) \right] \quad (32)$$

For the case of zero roughness (i.e. $\langle \alpha \rangle^2 = 0$) this expression reduces to Eq. (11) within the limits of the approximation Eq. (30).

Typical results from Eq. (31) are shown in Fig. 7 (in calculating these curves terms to second order in α were retained), indicating that the shape of the in-plane scattering patterns, and hence the position of the lobe peak, is not very sensitive to the value of the roughness parameter for $\langle \alpha \rangle^2 \frac{2}{5} \frac{MT_s}{mT_g} / \sin^2\theta_0 \left[1 + \frac{1+\mu}{2} \cot\theta(\cot\theta + \cot\theta_0) \right]^2$.

On the other hand, the half-width of the out-of-plane scattering is of order $2\langle \alpha \rangle$, and measurement of the out-of-plane scattering should be a useful way of investigating the surface roughness. The dashed line in Fig. 7 corresponds to the integrated case with $\langle \alpha \rangle = 0$, obtained from Eq. (32).

Similar curves are shown in Fig. 8, but in this case the parameter $\frac{MT_s}{mT_g}$ has been varied at fixed $\langle \alpha \rangle$. In this case the half-width of the out-of-plane scattering is not very sensitive to the value of $\frac{MT_s}{mT_g}$. In fact, in the lowest order approximation [Eq. (31)] the quantities

$$\frac{MT_s}{mT_g} \quad \text{and} \quad \phi \quad \text{are uncoupled.}$$

VI. Conclusions

The model presented here has the important attribute that it yields closed-form expressions for both the angular distribution and the speed distribution of gas atoms scattered from a solid surface. Due to the many simplifying assumptions, however, it is likely that the model becomes invalid when the following conditions apply: (a) the mass ratio is large, so that multiple collisions cannot be neglected, (b) the temperatures and masses are such that more than one solid atom effectively takes part in the collision ("slow" collision), (c) the energy of the incident atom is sufficient to displace the surface atom far from its equilibrium position, (d) the deBroglie wavelength of the gas atom is such that quantum-mechanical diffraction occurs, (e) the well-depth of the gas-surface potential is large compared to the incident energy, (f) the internal degrees of freedom (rotational, vibrational, and electronic) are affected by the collision. In general, we expect the model is best for the rare gases of thermal energy and with $\mu \lesssim 0.3$.

Some important characteristics of the results are as follows:

(1) The principal parameters of the scattering distribution are θ_0 , μ , and MT_s/mT_g . Hence, plots of θ_1 vs MT_s/mT_g (Fig. 2) should be a convenient means of correlating experimental data.

(2) The velocity distribution of scattered atoms is not Maxwellian, and the most probable velocity varies markedly with θ_1 .

(3) The out-of-plane width of the scattering patterns does not depend strongly on the gas or surface temperatures. The out-of-plane scattering should be a useful measure of the surface roughness.

Experimental investigation of these characteristics would be extremely valuable.

References

1. R. M. Logan and R. E. Stickney, *J. Chem. Phys.* **44**, 195, (1966).
2. F. O. Goodman, *J. Phys. Chem. Solids* **26**, 85 (1965).
3. H. Saltsburg and J. N. Smith, "Molecular Beam Scattering from the (111) Plane of Silver," General Atomic Report GA-6740, December 1965.

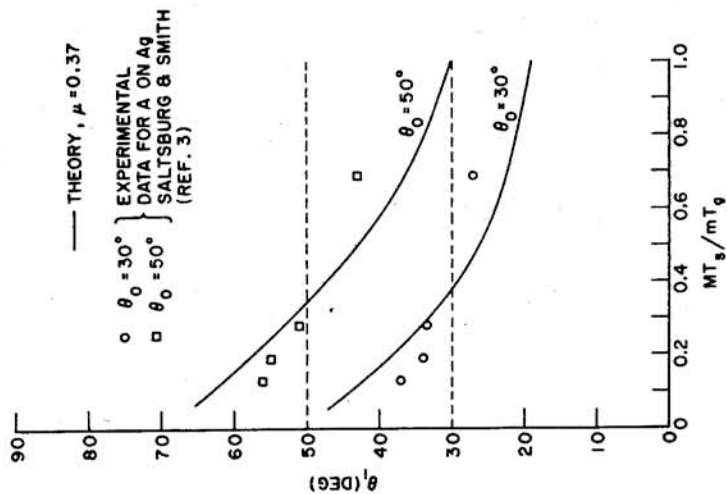


Fig. 2. Comparison of theoretical results [Eq. (11)] with experimental data for argon scattered from silver (reference 3).

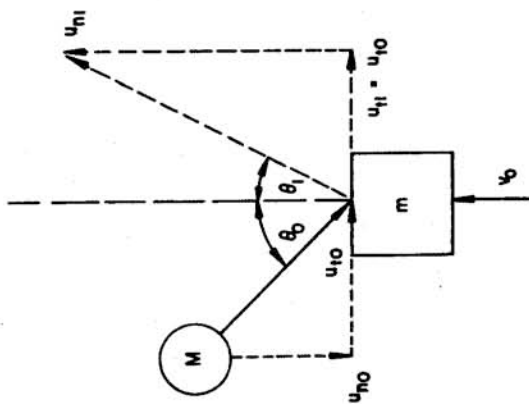


Fig. 1. Model for the collision of a gas atom of mass M with a surface atom of mass m .

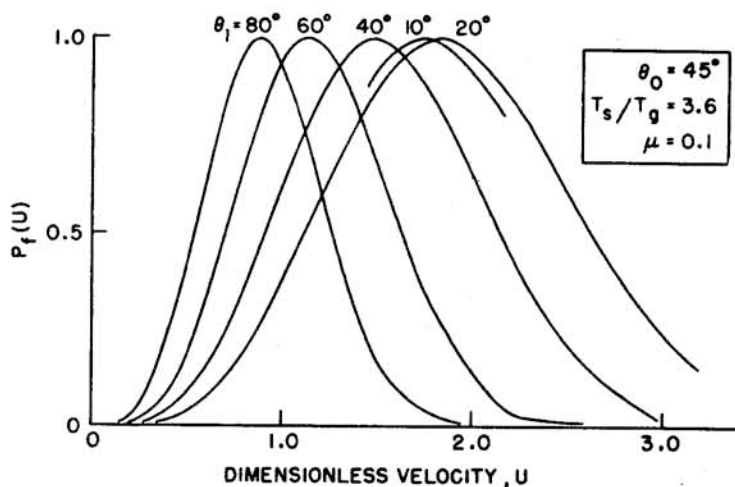


Fig. 3. Velocity distributions of the scattered gas atoms for various values of the outgoing angle θ_1 , calculated from Eq. (17).

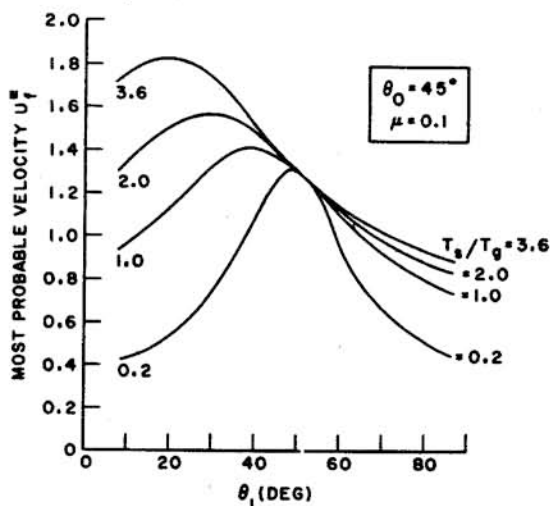


Fig. 4. Dependence of the most probable velocity of the scattered atoms U_f^* on outgoing angle θ_1 for various values of T_s/T_g , calculated from Eq. (19).

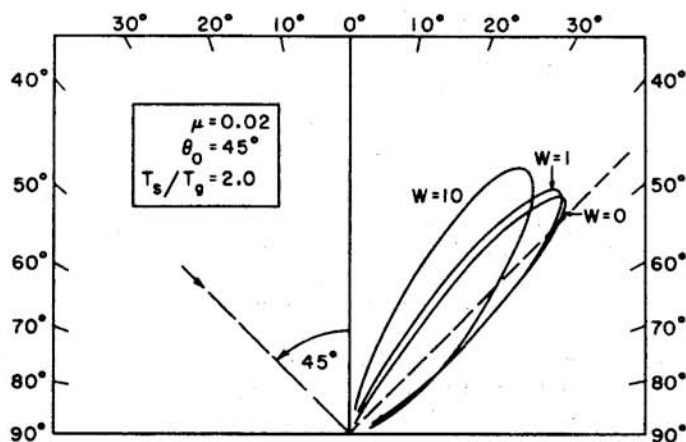


Fig. 5. Scattering patterns for various values of the well-depth parameter W .

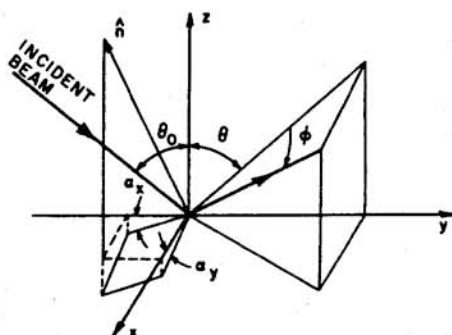


Fig. 6. Coordinate system for rough surface. The xy -plane represents the ideal flat surface, and \hat{n} represents the normal to the actual rough surface at the origin.

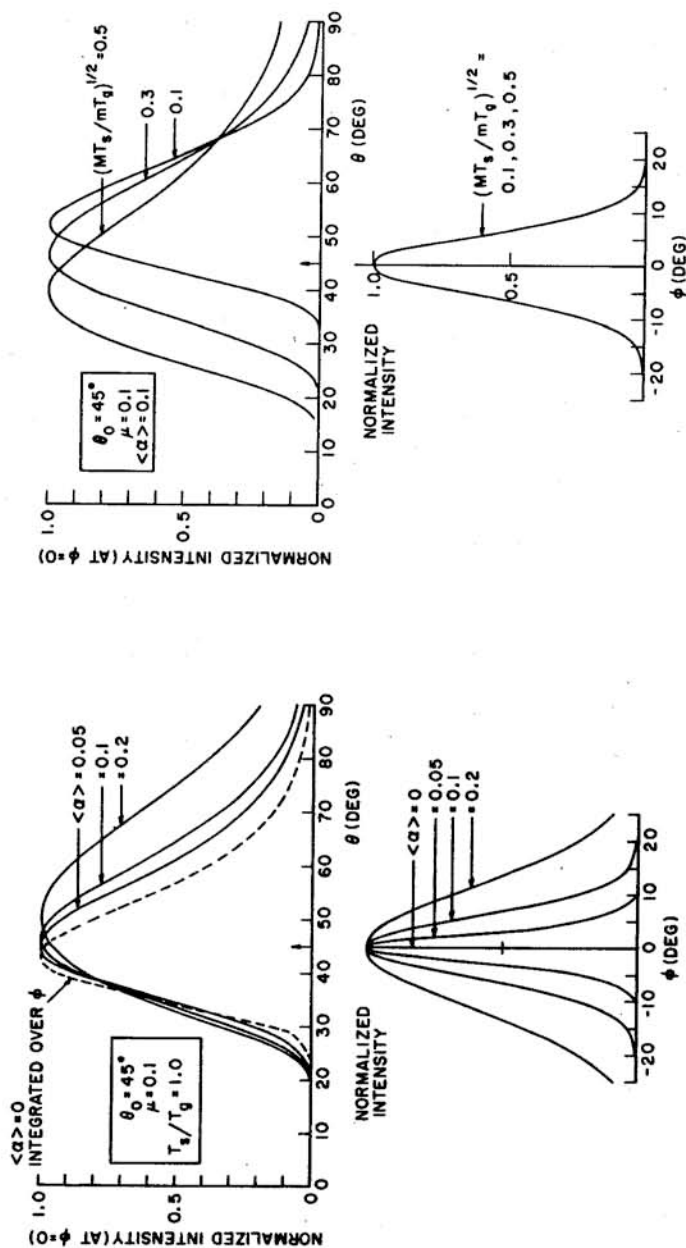


Fig. 7. Dependence of scattering patterns on the roughness parameter $\langle \alpha \rangle$, calculated from Eq. (31). The upper diagram shows the in-plane scattering patterns; the integrated curve is calculated from Eq. (32) for $\langle \alpha \rangle = 0$. The lower diagram shows the out-of-plane scattering, the intensities being the maxima occurring at each value of ϕ .

Fig. 8. Dependence of scattering patterns on $(M T_s / m T_g)^{1/2}$ for fixed $\langle \alpha \rangle$, calculated from Eq. (31). The upper diagram shows the in-plane scattering patterns. The lower diagram shows the out-of-plane scattering, the intensities being the maxima occurring at each value of ϕ .

DISCUSSION

KOGAN M.N. - In connection with last two very interesting reports I should like to point out some works, the ideas and results of which are close to the reported.

First of all I should like to refer the work of Frenkel, Ja.I. ("Uspekhi Fisicheskikh nauk" v. 20, N 1, 1938), in which he substantiated the validity of using the surface free atom model for the highly energetic incident molecules. This model was studied in detail by Barantsev R.G. (Symp. "Rarefied Gas Aerodynamics" v. 2, Ed. by Vallander S.V., Leningrad State Univ. Publ. House) for the closely packed surface atoms, and by Erofeev A.I. ("Ingenerni jurnal" v. 4, N 1, 1964) for the grid with the arbitrary pitch.

Erofeev A.I. ("Jurnal Prikladnoy mekhaniki y tekhnicheskoy fiziki", v. 2, N 3, 1966) also studied the interaction of diatomic molecules with the surface.

The effect of the roughness on the accommodation coefficient was considered by Barantsev R.G. (Symp. "Rarefied Gas Aerodynamics", v. 1, Ed. by Vallander S.V., Leningrad State Univ. Publ. House, 1964), and for the particular model - by Erofeev A.I. ("Ingenerni Jurnal", v. 5, N 5, 1965).